

Band-tail states and the localized-to-extended transition in amorphous diamond

Jianjun Dong and D. A. Drabold

Department of Physics and Astronomy, Condensed Matter and Surface Science Program, Ohio University, Athens, Ohio 45701-2979

(Received 8 July 1996)

The electronic structure of a large (4096 atom) and realistic model of amorphous diamond is studied. The density of states and the individual eigenstates in the valence-band tail and midgap region are computed with two “order- N ” spectral electronic-structure methods: the maximum entropy method and the shifted Lanczos method. We observe approximately exponential band tails at both valence- and conduction-band edges. The electronic states are explicitly computed in the vicinity of the gap through the valence-band tail region, and we track their spatial transition from highly local to extended. A simple model leading to exponential band tailing is described. [S0163-1829(96)08339-7]

One of the central issues of the physics of glassy and amorphous solids is the nature of the band tails in the electronic density of states (DOS). Particular issues include the following: (i) What is the origin of the ubiquitous exponential shape of the tails seen in photoemission and less directly in optical absorption measurements?¹ (ii) How does the spatial character of the electronic eigenstates change from the highly local midgap states to the extended states interior to the valence or conduction bands? The nature of the electronic states for electron energies ranging between midgap (localized) to valence or conduction (extended) is of obvious interest to the theory of doping and transport. The tools required to address such questions in an unambiguous way are the following.

(i) *Very large and realistic structural models of a representative amorphous system.* Small models can give a good account only of the the most highly localized midgap states, and necessarily fail in describing the spatial structure of the states as the volume of the state exceeds the volume of the supercell. Tantalizing hints of the nature of band tailing have been observed in earlier work on small supercells² and with elegant calculations using Bethe lattice techniques,³ which cannot provide a useful description of the spatial structure of the disorder-influenced electronic states. The structural model of this paper is a 4096-atom cubic supercell model of a -diamond (a -D) provided by Djordjevic *et al.*⁴ We note that a -D is a hypothetical, entirely fourfold material at a density of 3.52 gm/cm³ as crystalline diamond, but with topological (primarily bond angle) disorder. It is probably related to tetrahedral amorphous carbon (ta-C), which, however has a lower density (3.0 gm/cm³) and contains about 15% sp^2 sites.⁵ Column IV amorphous semiconductors a -Ge and a -Si are the materials most resembling a -D, with their large proclivity for sp^3 bonding (good quality unhydrogenated a -Si is believed to have less than 0.1% non- sp^3 sites). That the cell of Ref. 4 is a structurally credible model of amorphous diamond can be inferred from our local density approximation (LDA) relaxations of smaller versions (216- and 512-atom models) constructed in an analogous fashion with the Wooten-Weaire-Winer (WWW) method.⁶ We found that these smaller supercells of a -D were practically unchanged upon relaxation. We reported on this in more detail

elsewhere.⁷ At present, several thousand atom structural models are unattainable from *ab initio* molecular-dynamics simulations.

(ii) *Electronic structure methods able to cope with the large Hamiltonian matrices from which spectral information is required.* We use recently developed maximum entropy⁸ spectral methods^{9,10} to handle the state density calculations and a shifted Lanczos¹¹ scheme to compute the electronic states of interest from the sparse 16 384×16 384 Hamiltonian matrix. We use a block Lanczos method¹² and sparse matrix techniques to implement these calculations. We make the simplest reasonable choice of an electronic Hamiltonian: the orthogonal tight-binding Hamiltonian of Xu *et al.*¹³ For the *spectral* calculations we report here this Hamiltonian is a reasonable choice. Its reliability is also in little doubt for an entirely four-coordinated matrix as we study here. We concentrate on the valence-band tail in this paper since the basis of the Xu *et al.* Hamiltonian is minimal (one s and three p orbitals per site).

From a less applied point of view, this paper provides some information on the basic nature of electronic localization in three dimensions in the presence of topological disorder. Naturally, our calculations exhibit finite-size artifacts— since we restrict ourselves to a finite (albeit very large) system. Nevertheless, this work has the appeal of being more “realistic” (with genuine topological disorder as characterized by a fairly realistic Hamiltonian) than most of the large body of research applied to the celebrated Anderson model:¹⁴

$$H = \sum_{i=1}^n \varepsilon_i |i\rangle\langle i| + \sum_{\substack{i,j=1 \\ (i \neq j)}}^n V |i\rangle\langle j|, \quad (1)$$

in which, ε_i are random diagonal energies selected from a uniform distribution of width W and hopping parameter V is usually taken as constant. This diagonal disorder is more akin to “alloy disorder” than topological disorder in an elemental system for which the ε_i are identical for all sites and the disorder modulates V alone. In Eq. (1) the ratio W/V characterizes the degree of disorder of the model. An example of a recent study of the Anderson Hamiltonian for a very large system is the work of MacKinnon and Kramer,¹⁵

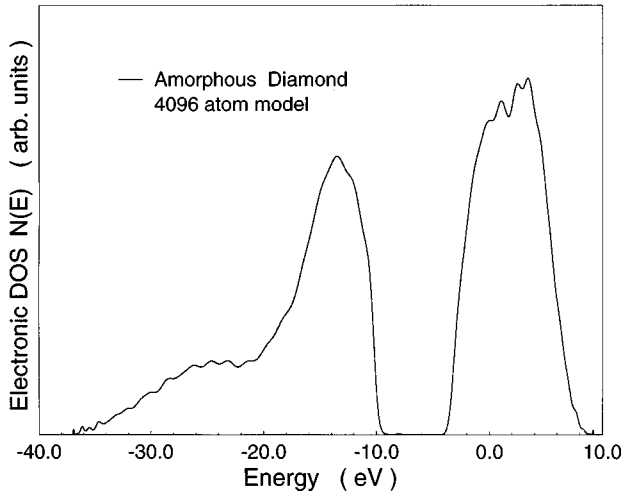


FIG. 1. Total electronic density of states (DOS) of amorphous diamond: 80 moments and 50 random vectors were used.

who compared their result with the scaling theory developed by Abrahams *et al.*¹⁶ The theory of localization for the Anderson model is a mature and sophisticated field, to which our calculations have some salience.

A variety of experiments on amorphous systems show the density of band tail states falling exponentially into the band gap.¹⁷ It is clear that both structural and thermal disorder contribute to the tail;² this work focuses on the structural origins of exponential tailing. Where structural broadening is concerned, an early argument of Halperin and Lax¹⁹ led to a DOS $N(E) \propto \exp(-\gamma|E|^{1/2})$ in three dimensions, and later Soukoulis *et al.*²⁰ modified the theory with scaling localization arguments and obtained the correct exponential form of the DOS. As a complement to this work, we give a simple argument below which also leads to exponential tails.

The electronic DOS of our amorphous diamond model is computed with the maximum entropy method⁹ and illustrated in Fig. 1. Compactly stated, random vectors and an averaging scheme are used to obtain up to 100 moments of the density of states of the sparse Hamiltonian matrix, and maximum entropy techniques are used to reconstruct the DOS from the moments. This procedure may be viewed as a maximum entropy “binning” of the (discrete) DOS. Care was taken to properly converge the results with respect to both the number of moments and random vectors.⁹ For an illustration of the spectral resolution this method affords, see Refs. 10 and 21. In Fig. 2(a) we show the valence-band edge region for diamond in a 4096-atom cell and the tails from the Djordjevic cell. The crystalline diamond cell has a defect-free gap with sharp band edge, while the amorphous diamond model has extended band tailing at both valence and conduction bands, as well as a few defect states in the middle of the band gap. Different numbers of moments and random vectors are used to compute the DOS. Figure 2(b) shows that our result of 80 moments and 50 vectors is well converged. These parameters, particularly the number of random vectors selected, is very conservative. A semilog plot in Fig. 3 reveals that the band tail falls approximately exponentially, which agrees with the experimental observation. The tail decay parameter E_0 [such that the valence DOS $\propto \exp(-E/E_0)$] is about 180 meV (versus approximately 60

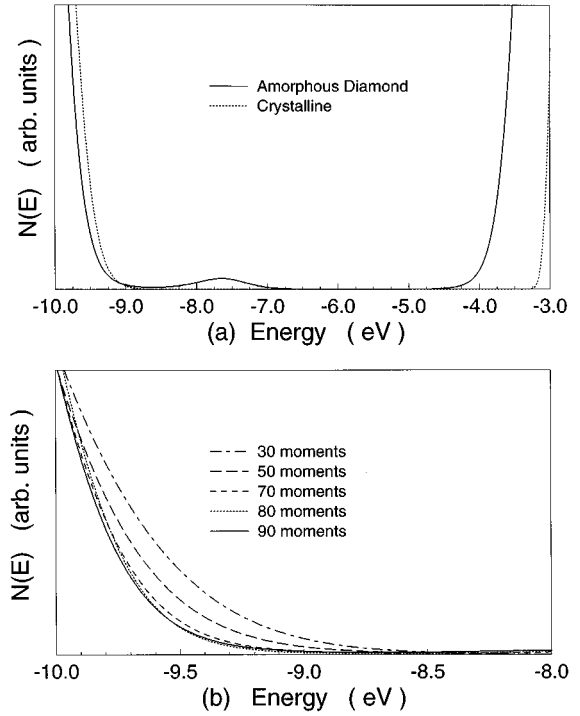


FIG. 2. (a) Electronic DOS in the band-gap region. The solid curve depicts *a*-D; dotted curve is crystalline diamond. (b) Results with different numbers of moments. Convergence of the maximum entropy reconstruction is obtained with 80 moments and 50 vectors.

meV seen in photoemission studies on *a*-Si).¹⁷ Experimental comparison to *a*-Si or *a*-Ge is necessarily qualitative.

We also find it useful to present a simple heuristic argument for the origin of structural exponential tailing for the valence edge based upon the following assumptions. First, as suggested by Bethe lattice calculations,³ we view band tailing as originating in bond angle distortions from the tetrahedral angle θ_T ; and we further assume that an energy deviation from the diamond valence edge value can be assigned

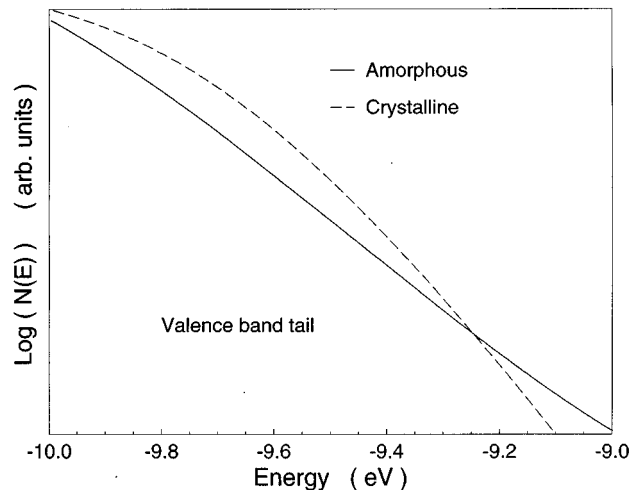


FIG. 3. Semilog plot of electronic DOS in the valence-band tail. The linearity of the graph for *a*-D suggests an exponential valence tail. The DOS changes by a factor of ≈ 150 over the range plotted.

associated with these distortions. This effectively assumes that the states in question are substantially localized (inhomogeneously broadened). Second, we have observed that the distribution of the cosine of bond angles θ in the cell is very well approximated with a normal distribution $p(\xi) = \exp[-(\xi - \xi_t)^2 / 2\sigma^2] / (2\pi\sigma^2)^{1/2}$ with $\xi = \cos(\theta)$, $\xi_t = \cos(109.01^\circ)$ (the mean bond angle is near θ_T , as expected), and $\sigma = 0.149$ (corresponding to a dispersion in θ of about 9.0°). This bond angle distribution was generated by the WWW method, and is seen in the smaller 216 and 512 models as well, and as we pointed out, *it is preserved under an LDA relaxation in 216- and 512-atom models*, lending some credence to the view that the normally distributed cosines are realistic at least for dominantly four-coordinated systems. To investigate this further, we would like to consider bond angle distributions in supercell models generated entirely from *ab initio* methods, but there are two problems with this: (i) the statistics are poor because of the small cell size and (ii) the unphysically large number of defects obtained in virtually all *ab initio* simulations introduces a complicating factor in interpreting the resulting distributions. With the assumption of normally distributed cosines, we take the crystalline valence-band edge to be at energy λ_V . As $\lambda(\xi)$ is presumably a minimum for $\xi_T = \cos(\theta_T) \approx \xi_t$, this function can be approximated for small distortions as $\lambda = \lambda_V + K(\xi - \xi_t)^2$, where K is a positive constant. As the probability density function (PDF) of $\xi = \cos\theta$ is normal, one can easily write the PDF for λ , the highest valence-band eigenvalue as broadened by the structural disorder of this model by using the usual rule for changing variables in a PDF. One obtains $N(\lambda) \propto \exp[-|\gamma(\lambda - \lambda_V)|]$ where $\gamma = (2\sigma^2 K)^{-1}$. An essentially identical argument can be stated for the conduction tail. We note that, in this simple picture, *any* mechanism causing approximately Gaussian bond angle disorder leads to exponential tails. Consider a very simplified model for the network dynamics, and assume the lattice is in thermal equilibrium at finite temperature T . In a valence force field model,¹⁸ the energy associated with bond bending involves a term of the form $U = \epsilon_0 [\delta\xi]^2$, where $\delta\xi$ is the deviation of the angle between adjacent bonds from ξ_T . Parameter ϵ_0 may be inferred from Ref. 18 for a variety of materials. If one neglects other distortions, comparison to the canonical distribution function suggests that thermal disorder leads to normally distributed cosines [with the width of the distribution $\sigma^2(T) \propto T$]. The resulting linear dependence in the exponential “tail width” is clearly seen in experiments for the conduction tail in Ref. 17 (for *a*-Si), and less obviously for the valence tailing, which seems to be mostly structural in origin.

To show the nature of these band tail states, we apply a shifted Lanczos method¹¹ to probe the midgap and valence tail energy region. We computed about 30 eigenstates in the valence-band tail. The localization is characterized by the inverse participation ratio (IPR) defined as: $I(\psi_j) = N \sum_{i=1}^N a_i^{j4} / \sum_{i=1}^N a_i^{j2}$ where $\psi_j = \sum_{i=1}^N a_i^j \phi_i$ is the j th eigenvector and $\{\phi_i\}$ is the (tight-binding) orthogonal basis and $N = 16\,384$, the number of basis functions. Note that $I = 1$ for completely uniform extended states and $I = N$ for a state completely localized on a single orbital: results are presented in Fig. 4. The first several defect states in the middle of the gap ($E \approx -8\text{ eV}$) are strongly localized. As the energy

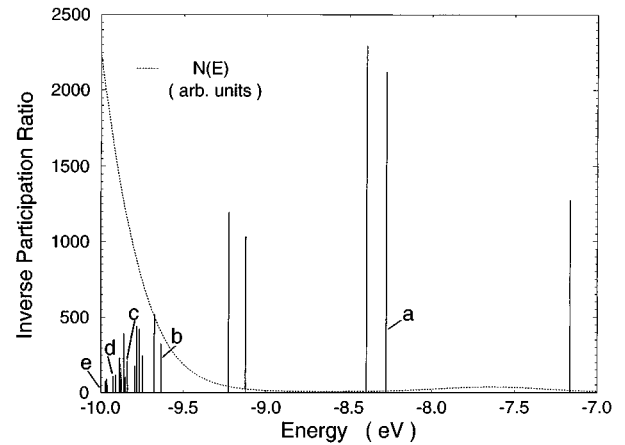


FIG. 4. DOS and localization as measured by the inverse participation ratio in the valence band tail region. The letters refer to Fig. 5.

approaches the interior of the valence band (from about -9 eV to about -10 eV), the degree of localization substantially decreases. This is more clearly shown in Fig. 5. Atoms are assigned different gray-scale renderings (darker more charge localization) according to their contribution to

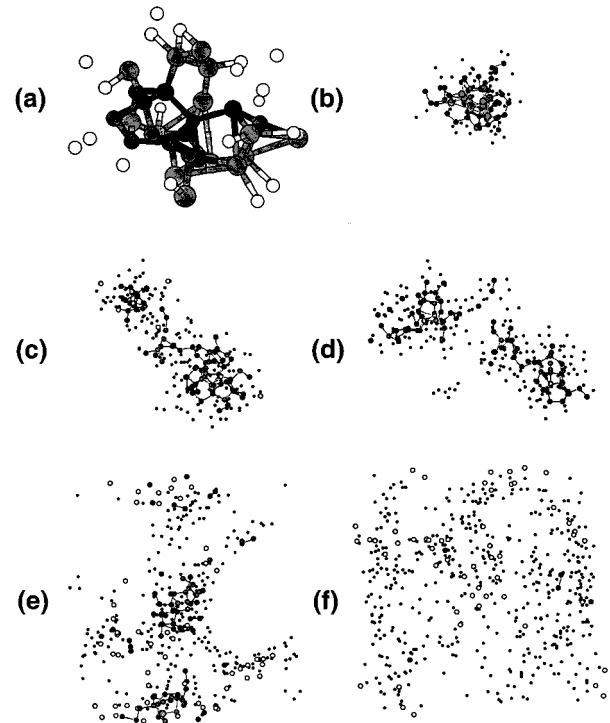


FIG. 5. Spatial character of the local to extended transition. Darker shading implies more charge localization. I is the inverse participation ratio (see text). (a) $E = -8.27\text{ eV}$: highly localized midgap state ($I = 2120$); (b) $E = -9.63\text{ eV}$: less compact cluster ($I = 326$); (c) $E = -9.84\text{ eV}$: larger cluster ($I = 210$); (d) $E = -9.92\text{ eV}$: weight on two separated clusters ($I = 110$); (e) $E = -10.0\text{ eV}$: nearly extended state ($I = 49$); (f) $E = -11.0\text{ eV}$: extended valence state ($I = 5$). Connecting lines between atoms depict bonds.

the eigenvectors. Atoms making little contribution (where $<0.05\%$ of the “charge” is located) are omitted in the figure. The origin of the midgap defect state [Fig. 5(a)] is found to be an atom that has very large bond angle distortion ($\Delta\theta\approx 20^\circ$). Such states are strongly localized on the defect core and its nearest neighbors. As we expect, such large angle distortions are rare in the model, so only a few (3 of 16 384) midgap states are found. States deeper into the band tail but tend to have weight on certain clusters of atoms. The deeper the state is inside the band, the larger the size of the cluster, which implies smaller IPR. There is an interesting pattern in which, when the size of the cluster increases to a certain point, the localized states start to “bifurcate” into two smaller weakly coupled pieces [compare Figs. 5(c) and 5(d)]. As we have pointed out elsewhere,²² using the simple language of perturbation theory, it is natural to see this as a “resonant phenomenon” in the sense that electronic states can spatially mix “energetically similar” parts of the network that are well separated in the supercell because of

“small energy denominators.” We have seen a very similar resonance effect on vibrational eigenstates in glassy GeSe₂.²³ As one progresses deeply into the valence tail, the fraction of the network associated with the given energy increases until the states become fully extended; for E close to -10 eV, there is no clear pattern of clustering and states become quite extended.

We would like to thank Dr. B. R. Djordjevic and Professor M. F. Thorpe for providing us with their structural model. We further thank Professor Ron Cappelletti, Professor Peter Fedders, Dr. Heinrich Röder, and Dr. R. N. Silver for helpful discussions. We would like to single out Professor G. R. Harp for his helpful comments leading to the geometrical/statistical argument for the origin of exponential tails. This work was partially supported by NSF under Grant No. DMR 93-22412 and the Ohio Supercomputer Center under Grant No. PHS218-1.

¹N.F. Mott and E.A. Davis, *Electronic Processes in Non-Crystalline Materials*, 2nd ed. (Clarendon, Oxford, 1979).

²D.A. Drabold *et al.*, Phys. Rev. Lett. **67**, 2179 (1991).

³See, for example, D. Allan and J. Joannopoulos, in *Hydrogenated Amorphous Silicon II*, edited by J. Joannopoulos and G. Lucovsky (Springer, Berlin, 1984) p. 5.

⁴B.R. Djordjevic *et al.*, Phys. Rev. B **52**, 5685 (1995)

⁵D.R. McKenzie *et al.*, Phys. Rev. Lett. **67**, 773 (1991).

⁶F. Wooten and D. Weaire, in *Solid State Physics: Advances in Research and Applications*, edited by H. Ehrenreich and D. Turnbull (Academic, New York, 1987), Vol. 40, p. 2.

⁷D.A. Drabold *et al.*, Phys. Rev. B **49**, 16 415 (1994).

⁸E.T. Jaynes, Phys. Rev. **106**, 620 (1957); *Papers on Probability, Statistics and Statistical Physics* (Kluwer, Dordrecht, 1983).

⁹D.A. Drabold and O.F. Sankey, Phys. Rev. Lett. **70**, 3631 (1993), and references therein.

¹⁰D.A. Drabold *et al.*, Solid State Commun. **96**, 833 (1995).

¹¹G. Grosso *et al.*, Il Nuovo Cimento D **15**, 269 (1993).

¹²G.H. Golub and C.F. Van Loan, *Matrix Computations* (Johns Hopkins University Press, Baltimore, 1983).

¹³C.H. Xu *et al.*, J. Phys. Condens. Matter **4**, 6047 (1992).

¹⁴P.W. Anderson, Phys. Rev. **109**, 1492 (1958).

¹⁵A. MacKinnon and B. Kramer, Z. Phys. B **53**, 1 (1983).

¹⁶E. Abrahams *et al.*, Phys. Rev. Lett. **42**, 673 (1979).

¹⁷For amorphous Si, see particularly S. Aljishi *et al.*, Phys. Rev. Lett. **64**, 2811 (1990), and references therein.

¹⁸R.M. Martin, Phys. Rev. B **1**, 4005 (1970).

¹⁹B.I. Halperin and M. Lax, Phys. Rev. **148**, 722 (1966); Phys. Rev. **153**, 802 (1967).

²⁰C.M. Soukoulis *et al.*, Phys. Rev. Lett. **53**, 616 (1984), and references therein.

²¹P. Ordejón *et al.*, Phys. Rev. Lett. **75**, 1324 (1995).

²²D.A. Drabold *et al.*, Phys. Rev. B **54**, 5480 (1996).

²³R.L. Cappelletti *et al.*, Phys. Rev. B **52**, 9133 (1995).